Improved Automated Optic Cup Segmentation Based on Detection of Blood Vessel Bends in Retinal Fundus Images

Yuji Hatanaka, *IEEE Member*, Yuuki Nagahata, Chisako Muramatsu, Susumu Okumura, Kazunori Ogohara, Akira Sawada, Kyoko Ishida, Tetsuya Yamamoto and Hiroshi Fujita, *IEEE Member*

***Abstract*— Glaucoma is a leading cause of permanent blindness. Retinal imaging is useful for early detection of glaucoma. In order to evaluate the presence of glaucoma, ophthalmologists may determine the cup and disc areas and diagnose glaucoma using a vertical optic cup-to-disc (C/D) ratio and a rim-to-disc (R/D) ratio. Previously we proposed a method to determine cup edge by analyzing a vertical profile of pixel values, but this method provided a cup edge smaller than that of an ophthalmologist. This paper describes an improved method using the locations of the blood vessel bends. The blood vessels were detected by a concentration feature determined from the density gradient. The blood vessel bends were detected by tracking the blood vessels from the disc edge to the primary cup edge, which was determined by our previous method. Lastly, the vertical C/D ratio and the R/D ratio were calculated. Using forty-four images, including 32 glaucoma images, the AUCs of both the vertical C/D ratio and R/D ratio by this proposed method were 0.966 and 0.936, respectively.**

I. Introduction

Glaucoma is the leading cause of blindness in Japan. The number of glaucoma patients is increasing in Japan with one in about 20 people over the age of 40 being diagnosed with glaucoma [1, 2]. However, about 90 percent of the patients are not diagnosed because many of them are asymptomatic in the early stage of the disease. If they were diagnosed earlier, then permanent blindness may be avoided. Thus, screening and periodical check-ups are important for the early diagnosis of glaucoma. But, many patients with glaucoma cannot be diagnosed by using only ophthalmotonometry because 3.6 percent of the people have normal tension glaucoma (NTG) [1, 2]. Moreover, it is difficult diagnose glaucoma because of the need to conduct several ophthalmological examinations, including ophthalmotonometry, funduscopy, visual field examination, etc., in mass screening. Retinal imaging is an easy and effective diagnostic exam. The findings indicating glaucoma in the retinal image are large cupping, rim loss, rim notching, peripapillary atrophy (PPA), nerve fiber layer defects (NFLDs), etc. Large cupping is found by measuring the vertical optic cup-to disc (C/D) ratio, and rim loss is found by measuring the rim-to-disc (R/D) ratio. Although the use of retinal imaging has improved ocular healthcare, the number of ophthalmologists has not increased, thus increasing their workload. Computer-aided diagnosis (CAD) systems, developed for analyzing retinal images, can assist in both reducing the workload of ophthalmologists and improving the screening accuracy.

The purpose of this study is to analyze the optic disc on a retinal image, which is important for diagnosis of glaucoma. Three-dimensional images captured on a stereo retinal fundus camera [3-8] and HRT [9] were used in several studies. However, it is still difficult to use such 3D retinal fundus camera in the screening. Thus, we attempted to measure the vertical C/D and R/D ratios automatically using two-dimensional retinal images. Several studies have also reported on automated C/D ratio measurements [10-12]. Joshi et al proposed an automated cup and disc segmentation [10]. The disc was segmented using an active contour model (ACM), and the cup was segmented using r-bends information. Cheng et al proposed segmentation of the cup and disc using a superpixel classification with the histograms, the center surround statistics, and the location information [11]. We also proposed an automated cup and disc segmentation [12]. The disc was segmented using ACM [13]. Since we thought that the detection of blood vessel bends (kinks) was very difficult, we segmented the cup using profile analysis based on the blue image channel [12]. Our previous method detected bright region as the cup region, but bright region tended to smaller region than the cup region determined by expert ophthalmologists. Experts determine a cup edge by reference of the blood vessel bends on an optic disc region. Thus, our method found some vertical C/D ratios that were smaller than those determined by ophthalmologists, and the area under the curve (AUC) was 0.87 in receiver operating characteristic (ROC) [12]. The purpose of this study is to improve a cup contour detection by automatic detection of blood vessel bends.

II. Methods

Retinal images were captured using a retinal fundus camera (Kowa VX-10i). The photographic angle of the fundus camera was set to 27 degrees, and the optic disc was set in the center of image. The retinal images were obtained with an array size of 1600 × 1200 pixels and 24-bit color. Our method consists of three steps; A) optic disc segmentation, B) cup segmentation, and C) determination of vertical C/D and R/D ratios. More details are given below.

A. Optic disc segmentation

In this study, the optic disc was segmented by our

This work was supported by the Adaptable and Seamless Technology Transfer Program through the target-driven R&D, Japan Science and Technology Agency (JST).

Y. Hatanaka, S. Okumura and K. Ogohara are with the Department of Electronic Systems Engineering, School of Engineering, the University of Shiga Prefecture, 2500 Hassaka-cho, Hikone-shi, Shiga 522-8533, Japan (phone: 81-749-28-9556; fax: 81-749-28-9576; e-mail: hatanaka.y@usp.ac.jp)

Y. Nagahata is a graduate student in the Division of Electronic Systems Engineering, Graduate School of Engineering, the University of Shiga Prefecture, 2500 Hassaka-cho, Hikone-shi, Shiga 522-8533, Japan.

C. Muramatsu and H. Fujita are with the Department of Intelligent Image Information, Graduate School of Medicine, Gifu University, 1-1 Yanagido, Gifu-shi, Gifu 501-1194, Japan.

A. Sawada and T. Yamamoto are with the Department of Ophthalmology, Graduate School of Medicine, Gifu University, 1-1 Yanagido, Gifu-shi, Gifu 501-1194, Japan.

K. Ishida is with the Department of Ophthalmology, Toho University Ohashi Medical Center, 2-17-6 Ohashi, Meguro-ku, Tokyo 153-8515, Japan.

978-1-4244-7929-0/14/$26.00 ©2014 IEEE

proposed method based on ACM [13]. The blood-vessel-erased image was first created by using our proposed method [14]. Forty eight initial candidate points on the disc edges were selected on the basis of the edges identified by applying the Canny edge detector on the red channel of the blood-vessel-erased images. The candidate points were updated by the active contour modeling. The outline of the optic disc was determined using the spline interpolation method. The mean error in the largest vertical lengths of the disc regions was 4.5% [13].

B. Cup segmentation

The initial cup outline was determined by our previous method [12], and the details are given below. Since there is high contrast between the cup and rim regions in the blue channel of a color blood-vessel-erased image [14], a profile in the blue channel was then obtained around the center of gravity of the disc region. Subsequently, the cup edge was determined by using the zero-crossing method. By obtaining the profiles around the center of gravity of the disc region, the omniazimuth cup edge candidates were obtained. The initial cup outline was determined by the spline interpolation method based on the omniazimuth cup edge candidates.

Our previous method [12] detected the blood vessel regions using the black-top-hat. But, the black-top-hat could not detect the blood vessel regions with low contrast. Thus, we propose that blood vessel detection be based on the concentration feature determined from the density gradient [15]. The concentration feature $G(i, j, R)$ is

$$G(i,j,R) = \Sigma_{x,y \in R} d(x,y) f(x,y) \quad (1)$$

where i and j are image coordinates, R is the radius of calculation mask, $d(x, y)$ represents the intensity component in the Sobel filter, and $f(x, y)$ is given by the following:

$$f(\mathrm{x},\mathrm{y}) = \cos[\,\theta(x,y) + n \cdot \sin\{2\theta(x,y) - \pi\}\,] \quad (2)$$

where $\theta(x,y)$ is the difference between the Sobel gradient direction $\vec{D}$ and the direction of (x,y) and the center of R as shown in Fig. 1. Since $f(\mathrm{x},\mathrm{y})$ is influenced by the direction component of the density gradient, it increases when the direction component turns to the center of the mask. From the definition above, it is noted that $d(x,y)f(x,y)$ becomes greater when the direction of the density gradient turns to the center of the mask and the value of the density gradient becomes larger. In (2), "n" is a fixed number, and the value of 0.2 for "n" was determined experimentally. The sin term is added inside the cos term so that a few changes of $\theta(x,y)$ will not influence $f(\mathrm{x},\mathrm{y})$ greatly [15]. In this study, the maximum value of $G(i,j,9)$, $G(i,j,11)$ and $G(i,j,13)$ is determined as a final concentration $C(i,j)$.

$$C(i,j) = \max_{R=9,11,13} G(i,j,R) \quad (3)$$

The retinal image was filtered by $C(i,j)$ (as shown in Fig.2 (b)), and then the blood vessels were detected by the p-tile method, as shown in Fig. 2 (c).

The blood vessel bends were detected by tracking the blood vessels from the disc outline to the initial cup outline. We divided the bends into 2 types, visible bend and invisible bend going backward, as shown in Fig. 3. The visible bends were

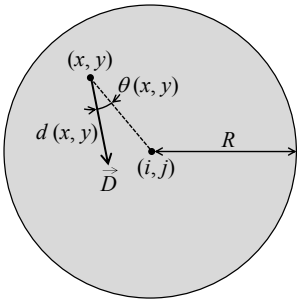

Figure 1. Elements for calculating the concentration. $d(x,y)$ represents the intensity component of the density gradient. The value of $\theta(x,y)$ shows the angle determined by the direction from the center of the mask to point (x,y) and the direction of the density gradient. D : density gradient vector.

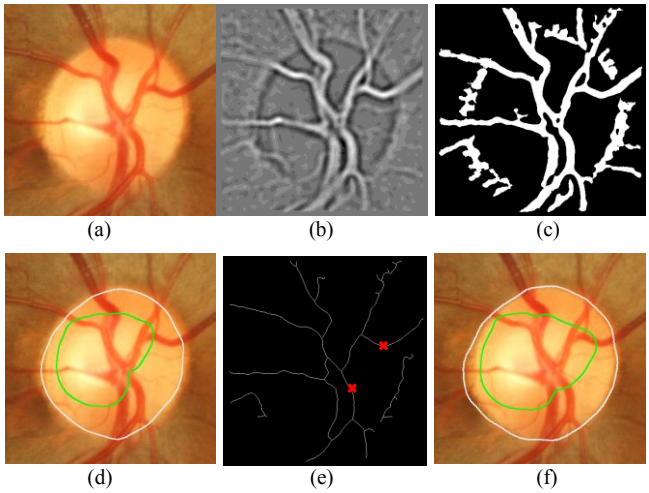

Figure 2. Example of blood vessel detection and blood vessel bend detection. (a) Original retinal image. (b) The image was filtered by the concentration. (c) The blood vessel regions were segmented using the p-tile method. (d) The inner ring shows the initial cup outline. The outer ring shows the optic disc outline. (e) The x- marks show the bends. (f) The result of cup and disc outlines.

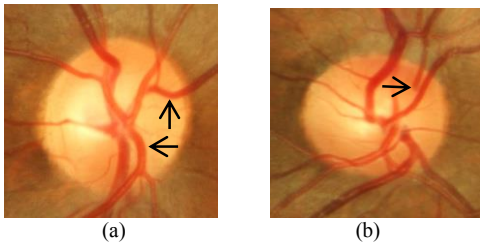

Figure 3. Two types of blood vessel bends. The arrows show (a) visible bends and (b) invisible bend going backward.

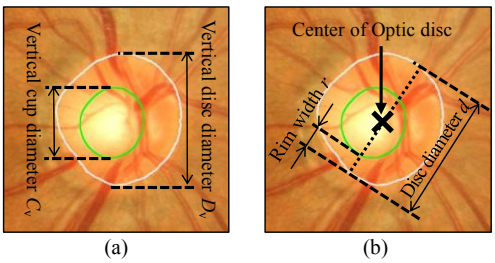

Figure 4. Determination of (a) C/D ratio and (b) R/D ratio.

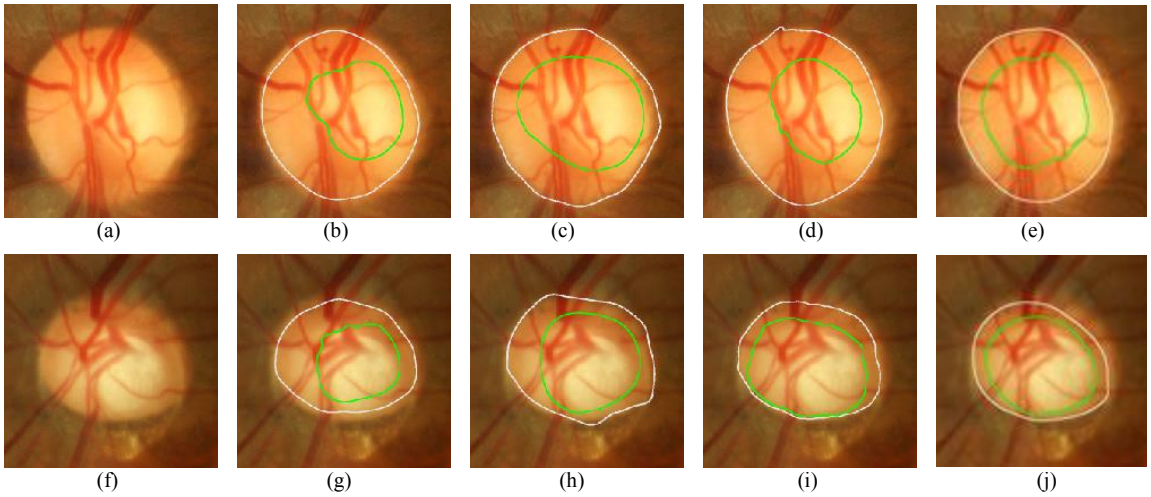

Figure 5. Examples of results. (a) to (e) show normal images. (f) to (j) show glaucoma images. (a) and (f) are original images. (b) and (g) are the results using the previous method, (c) and (h) are the results using the proposed method, (d) and (i) are sketches by an ophthalmologist 1, (e) and (j) are sketches by an ophthalmologist 2.

TABLE I. CDR AND RDR OF THE NORMAL IMAGE

	Proposed	Previous	Ophthalmologist 1	Ophthalmologist 2
CDR	0.67	0.58	0.59	0.66
RDR	0.11	0.11	0.16	0.14

TABLE II. CDR AND RDR OF THE GLAUCOMA IMAGE

	Proposed	Previous	Ophthalmologist 1	Ophthalmologist 2
CDR	0.76	0.69	0.84	0.84
RDR	0.06	0.08	0.01	0.04

detected by the k-curvature [16]. The invisible bends looked like endpoints on the optic disc, thus such endpoints were detected as the bends. The cup edge candidates were updated by using the bends. The outline of the cup was finally determined using the spline interpolation method.

C. Determination of vertical C/D and R/D ratios

The vertical C/D ratio CDR was determined by the method of Gloster et al [17]:

$$\mathrm{CDR} = C_v / D_v \tag{4}$$

where C_v is the vertical cup diameter, and D_v is the vertical disc diameter. C_v and D_v were determined by the distances between the top and bottom levels of these diameters (as shown in Fig. 4). The higher the CDR is, the higher the glaucoma risk is. In upper (11-1 o'lock hours) or lower (5-7 o'clock hours) of the disc, the narrowest dimension r of the rim divided by the diameter d of the disc at that point was determined as the R/D ratio RDR [17].

$$\mathrm{RDR} = r / d \tag{5}$$

The lower the RRD is, the higher the glaucoma risk is.

III. RESULTS AND DISCUSSION

The proposed method for measurement of CDR and RDR was evaluated on the basis of the manual outlines drawn by two ophthalmologists, who are experts in glaucoma diagnosis. Two ophthalmologists classified 50 retinal images into glaucoma and normal, and 44 retinal images were agreed by both. Thus, we used 44 retinal images, including 32 glaucoma images, in this test.

The examples of the cup and disc outlines determined by the proposed method, previous method, and 2 ophthalmologists in both normal and glaucoma images are shown in Fig. 5, respectively. The CDR and RDR measured in the normal image of Fig. 5 (a) are shown in TABLE I. The cup region determined by the proposed method was larger toward right and left than that determined by the ophthalmologist, because the proposed method detected the bend of the thin blood vessel in the left side of the optic disc. However, the upper cup edge and the lower cup edge determined by the proposed method were similar to them of 2 ophthalmologists. Thus, the CDR and RDR were both in the range of normal. The CDR and RDR measured in glaucoma image of Fig. 5 (e) are shown in TABLE II. The cup region determined by the previous method was small, but that determined by the proposed method was improved and similar to them of 2 ophthalmologists. Moreover, the CDR determined by the previous method was in the range of normal, but that determined by the proposed method was in the range of glaucoma.

We then analyzed the results of the CDR and RDR using ROC (receiver operating characteristic) analysis, as shown in Fig. 6 and Fig. 7, respectively. Note that the difference is very small because of the curve fitting. The area under the curves (AUC) by the CDRs of the proposed method and the previous method were 0.966 and 0.965, respectively. But, the sensitivities by the previous method and the proposed method were 46.9% and 62.5%, respectively, when both specificities were 100%. The AUC of the RDR determined by the proposed method and the previous method were 0.936 and 0.896, respectively. Moreover, the sensitivity by the proposed method was jumped 56.3% to 78.1%, when both specificities were 91.7%. Thus, the performance of the RDR determined by the proposed method was higher than that of previous one. Although the cup regions by the proposed method were slightly small, the proposed method indicated that it can be useful for automatic measurement of the CDR and the RDR.

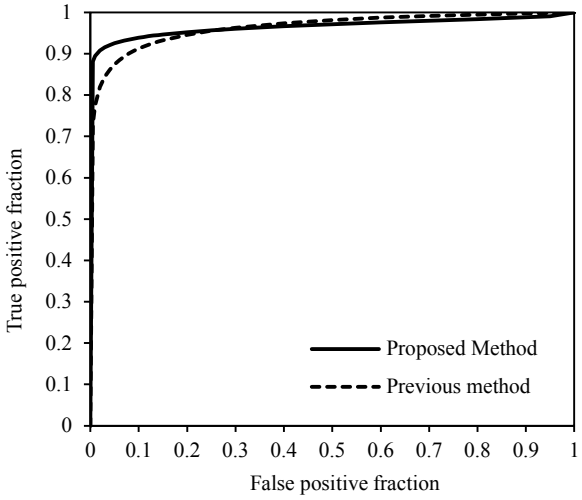

Figure 6. ROC curves by CDR of both the previous method and the proposed method are shown.

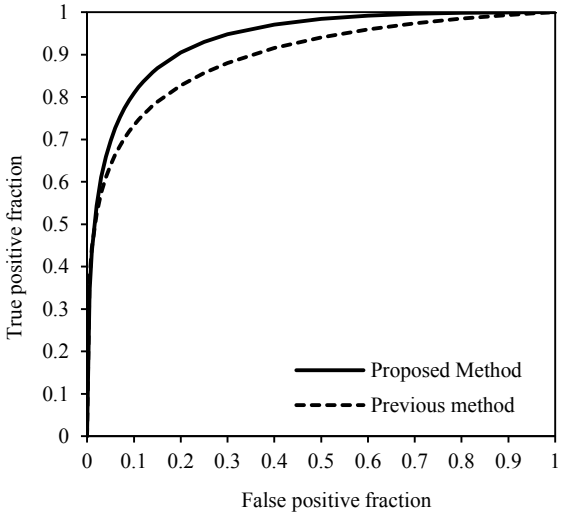

Figure 7. ROC curves by RDR determined by the previous method and by the proposed method are shown.

The AUCs of the CDR and the RDR determined by 2 ophthalmologists were all 1.00. Thus, his measurement was too high. In the future, we plan to have either a resident or an inexperienced ophthalmologist perform the measurement.

IV. Conclusion

We proposed a measurement method for the vertical C/D ratio and R/D ratio based on a determination of the cup edge in retinal images. The cup outline was improved by the detection of blood vessel bends. The AUCs of the vertical C/D ratio and R/D ratio determined by the proposed method reached 0.966 and 0.936, respectively. Although the proposed method is not error-free, the results indicated that it can be useful.

Acknowledgment

The authors thank R. Shiraki, T. Nakagawa, K. Fukuta, A. Noudo and M. Akao for their significant contributions to this study.

References

[1] A. Iwase, Y. Suzuki, M. Araie, T. Yamamoto, H. Abe, S. Shirato, Y. Kuwayama, H. Mishima, H. Shimizu, and G. Tomita, "The Prevalence of Primary Open-Angle Glaucoma in Japanese: The Tajimi Study", *Ophthalmology*, vol. 111, no. 9, pp. 1641–1648, Sep. 2004.

[2] T. Yamamoto, A. Iwase, M. Araie, Y. Suzuki, H. Abe, S. Shirato, Y. Kuwayama, H. Mishima, H. Shimizu, and G. Tomita, "The Tajimi Study Report 2 Prevalence of Primary Angle Closure and Secondary Glaucoma in a Japanese Population", *Ophthalmology*, vol. 112, no. 10, pp. 1661–1669, Oct. 2005.

[3] T. Nakagawa, T. Suzuki, Y. Hayashi, Y. Mizukusa, Y. Hatanaka, K. Ishida, T. Hara, H. Fujita, and T. Yamamoto, "Quantitative Depth Analysis of Optic Nerve Head Using Stereo Retinal Fundus Image Pair", *J. Biomedical Optics*, vol. 13, no. 6, pp. 064026 (10 pages), Dec. 2008.

[4] C. Muramatsu, Y. Hatanaka, K. Ishida, A. Sawada, T. Yamamoto, and H. Fujita, "Preliminary Study on Differentiation between Glaucomatous and Non-glaucomatous Eyes on Stereo Fundus Images Using Cup Gradient Models", *Proc. SPIE*, vol. 9035, in press, Feb. 2014.

[5] M.B. Merickel X. Wu, M. Sonka, and M.D. Abramoff, "Optimal Segmentation of the Optic Nerve Head from Stereo Retinal Images", *Proc. SPIE*, vol. 6143, pp. 61433B (8 pages), Mar. 2006

[6] J. Xu, H. Ishikawa, G. Wollstein, R.A. Bilonick, K.R. Sung, L. Kagemann, K. A. Townsend, and J. S. Schumanl, "Automated Assessment of the Optic Nerve Head on Stereo Disc Photographs", *Investigative Ophthalmology & Visual Science*, vol. 49, no. 6, pp. 2512-7, June 2008.

[7] M.D. Abramoff, W.L.M. Alward, E. C.Greenlee, L.Shuba, C.Y. Kim, J.H. Fingert, and Y.H. Kwon, "Automated Segmentation of the Optic Disc from Stereo Color Photographs Using Physiologically Plausible Features", *Investigative Ophthalmology & Visual Science*, vol. 48, no. 4, pp. 1665-73, Apr. 2007.

[8] E. Corona, S. Mitra, M. Wilson, T. Krile, Y.H. Kwon, and P. Soliz, "Digital Stereo Image Analyzer for Generating Automated 3-D Measures of Optic Disc Deformatin in Glaucoma", *IEEE Trans Med. Imag.*, vol. 21, no. 10, pp. 1244–1253, Oct. 2002.

[9] F.S. Mikelberg, C.M. Parfitt, N.V. Swindale, S.L. Graham, S.M. Drance, and R. Gosine, "Ability of the Heidelberg Retina Tomograph to Detect Early Glaucomatous Visual Field Loss", *J. Glaucoma*, vol. 4, no. 4, pp. 242–247, Aug. 1995.

[10] G.D. Joshi, J. Sivaswamy, and S.R. Krishnadas, "Optic Disk and Cup Segmentation From Monocular Color Retinal Images for Glaucoma Assessment", *IEEE Trans Med. Imag.*, vol.30, no. 6, pp. 1192-1205, May, 2011.

[11] J. Cheng, J. Liu, Y. Xu, F. Yin, D.W.K. Wong, N. Tan, D. Tao, C. Cheng, T. Aung, and T. Y. Wong, "Superpixel Classification Based Optic Disc and Optic Cup Segmentation for Glaucoma Screening," *IEEE Trans Med. Imag.*, vol.32, no. 6, pp. 1019-1032, June 2013.

[12] Y. Hatanaka, A. Noudo, C. Muramatsu, A. Sawada, T. Hara, T. Yamamoto, and H. Fujita, "Automatic Measurement of Cup to Disc Radio Based on Line Profile Analysis in Retinal Images," *Proc. 33rd IEEE Eng. Med. Bio. Sci*., pp. 3387-3390, Aug. 2011.

[13] C. Muramatsu, T. Nakagawa, A. Sawada, Y. Hatanaka, T. Hara, T. Yamamoto, and H. Fujita, "Automated Segmentation of Optic Disc Region on Retinal Fundus Photographs: Comparison of Contour Modeling and Pixel Classification Methods", *Computer Methods and Programs in Biomedicine*, vol. 101, no. 1, pp. 23-32, Jan. 2011.

[14] T. Nakagawa, Y. Hayashi, Y. Hatanaka, A. Aoyama, Y. Mizukusa, A. Fujita, M. Kakogawa, T. Hara, H. Fujita, and T. Yamamoto, "Recognition of Optic Nerve Head Using Blood-Vessel-Erased Image and Its Application to Production of Simulated Stereogram in Computer-Aided Diagnosis System for Retinal Images", *IEICE Trans. Info.Systems*, vol. J89-D, no. 11, pp. 2491–2501, Nov. 1, 2006.

[15] Y. Hatanaka, T. Hara, H. Fujita, S. Kasai, T. Endo, and T. Iwase, "Development of an Automated Method for Ddetecting Mammographic Masses with a Partial Loss of Region, " *IEEE Trans Med. Imag.*, vol. 20, no. 12, pp. 1209-1214, Nov. 2001.

[16] B. Rosenberg, The analysis of convex blobs. Computer Graphics and Image Processing, Vol. 1, No.2, pp. 183-192, 1972.

[17] J. Gloster, and D.G. Parry, "Use of Photographs for Measuring Cupping in the Optic Disc", *Brit. J. Ophthalmology*, vol. 58, no. 10, pp.850-862, Oct. 1974.